Information-Energy Trade-offs with EH Non-linearities in the Finite Block-Length Regime with Finite Constellations

Sadaf Ul Zuhra, Samir M Perlaza, H Vincent Poor, Mikael Skoglund

Information-Energy Trade-offs with EH Non-linearities in the Finite Block-Length Regime with Finite Constellations

Sadaf ul Zuhra, Samir M. Perlaza, H. Vincent Poor, and Mikael Skoglund

***Abstract*—This paper characterizes the trade-offs between the information and energy transmission rates, the decoding error probability, and the energy outage probability in simultaneous information and energy transmission over an additive white Gaussian noise channel. The results in this paper take into account the impact of energy harvester (EH) non-linearities on the harvested energy. The analysis is carried out in the finite block-length regime with finite constellations. Improved converse and achievability bounds that account for the EH non-linearities are presented.**

I. Introduction

Simultaneous information and energy transmission (SIET) has emerged as a key enabler for the sixth generation (6G) [1] of wireless communication systems. SIET provides the means of remotely energizing low-power devices such as sensors and actuators using information-carrying radio frequency (RF) signals, thus relieving these devices from their dependence on manual battery re-charging. Most existing works in this area, *e.g.* [2]–[8], consider SIET in the asymptotic block-length regime. In this case, the decoding error probability (DEP) and the energy outage probability (EOP) can be made arbitrarily close to zero. However, in the finite block-length regime, which is the subject of this paper, the DEP and EOP are bounded away from zero. Earlier research on SIET in the finite block-length regime can be found in [9]–[12]. This work builds upon the work of [11] and [12] by accounting for the impact of the rectenna non-linearities [13]–[16] on the expected energy harvested from an RF signal. The trade-offs between the information and energy rates, DEP, and EOP are also characterized.

A. System Model

The system consists of a transmitter, an information receiver (IR), and an energy harvester (EH). The objective of the transmitter is to simultaneously send information to the IR at a rate of R bits per second; and energy to the EH at a rate of B Joules per second over an additive white Gaussian noise (AWGN) channel. The transmission takes place over a finite duration of $n \in \mathbb{N}$ channel uses. The transmitter uses L symbols from the set

$$\mathcal{X} \triangleq \{x^{(1)}, x^{(2)}, \ldots, x^{(L)}\} \subset \mathbb{C} \tag{1}$$

that contains all possible channel input symbols. That is,

$$L \triangleq |\mathcal{X}|. \tag{2}$$

For all $m \in \{1, 2, \ldots, n\}$, denote by $\nu_m \in \mathcal{X}$, the symbol to be transmitted during channel use m. Denote the vector of channel input symbols over n channel uses by

$$\boldsymbol{\nu} = (\nu_1, \nu_2, \ldots, \nu_n)^{\mathsf{T}}. \tag{3}$$

The baseband frequency of the transmitter in Hertz (Hz) is denoted by f_w. Denote by $T = \frac{1}{f_w}$, the duration of a channel use in time units. Hence, the transmission takes place during nT time units. The complex baseband signal at time t, with $t \in [0, nT]$ is given by

$$x(t) = \sum_{m=1}^{n} \nu_m \operatorname{sinc}\left(f_w \left(t - (m-1)T\right)\right), \tag{4}$$

where the notation sinc represents the normalized cardinal sine function [17, (5.20)]. The signal $x(t)$ in (4) has a bandwidth of $\frac{f_w}{2} > 0$ Hz. Let $f_c > \frac{f_w}{2}$ denote the center frequency of the transmitter. The RF signal input to the channel at time t, denoted by $\tilde{x}(t)$, is obtained by the frequency up-conversion of the baseband signal $x(t)$ in (4) as follows:

$$\tilde{x}(t) = \Re\left(x(t)\sqrt{2}\exp(\mathrm{i}2\pi f_c t)\right), \tag{5}$$

where i is the complex unit. The RF outputs of the AWGN channel at time $t \in [0, nT]$ are the random variables

$$Y(t) = \tilde{x}(t) + N_1(t), \text{ and} \tag{6a}$$

$$Z(t) = \tilde{x}(t) + N_2(t), \tag{6b}$$

where, for all $t \in [0, nT]$, the random variables $N_1(t)$ and $N_2(t)$ represent real white Gaussian noise with zero mean and variance σ^2. $Y(t)$ and $Z(t)$ are the inputs to the IR and the EH, respectively.

At the IR, the received signal $Y(t)$ in (6a) is first multiplied with $\sqrt{2}\exp(-\mathrm{i}2\pi f_c t)$ to obtain the down-converted output. The down-converted output is then passed through a unit gain low pass filter with impulse response $f_w \operatorname{sinc}(f_w t)$ that has a cut-off frequency of $\frac{f_w}{2}$ Hz to obtain the complex

Sadaf ul Zuhra and Samir M. Perlaza are with INRIA, 2004 Route des Lucioles, 06902 Sophia Antipolis, France. ({sadaf-ul.zuhra, samir.perlaza}@inria.fr)

H. Vincent Poor, Sadaf ul Zuhra, and Samir M. Perlaza are with the Department of Electrical and Computer Engineering, Princeton University, 08540 Princeton, NJ, USA. (poor@princeton.edu)

Mikael Skoglund is with the School of Electrical Engineering and Computer Science, Malvinas Väg 10, KTH Royal Institute of Technology, 11428 Stockholm, Sweden. (skoglund@kth.se)

Samir M. Perlaza is also with the Laboratoire de Mathématiques GAATI, Université de la Polynésie Française, BP 6570, 98702 Faaa, French Polynesia.

This research was supported in part by the European Commission through the H2020-MSCA-RISE-2019 program under grant 872172; in part by the Agence Nationale de la Recherche (ANR) through the project MAESTRO-5G (ANR-18-CE25-0012); in part by the U.S. National Science Foundation under Grant CCF-1908308; and in part by the French Government through the "Plan de Relance" and "Programme d'investissements d'avenir".

baseband equivalent of $Y(t)$. This is followed by ideally sampling the complex baseband output at intervals of $1/f_w$. The resulting discrete time baseband output at the end of n channel uses is given by the following random vector [18, Section 2.2.4]:

$$\boldsymbol{Y} = \boldsymbol{\nu} + \boldsymbol{N}, \tag{7}$$

where the vector $\boldsymbol{Y} = (Y_1, Y_2, \ldots, Y_n)^{\mathsf{T}} \in \mathbb{C}^n$ is the input to the IR; $\boldsymbol{\nu}$ is the vector of channel input symbols in (3); and $\boldsymbol{N} = (N_1, N_2, \ldots, N_n)^{\mathsf{T}} \in \mathbb{C}^n$ is the noise vector such that, for all $m \in \{1, 2, \ldots, n\}$, the random variable N_m is a complex circularly symmetric Gaussian random variable whose real and imaginary parts have zero means and variances $\frac{1}{2}\sigma^2$. Moreover, the random variables $N_1, N_2, \ldots, N_n$ are mutually independent (see [18, Section 2.2.4]). That is, for all $\boldsymbol{y} = (y_1, y_2, \ldots, y_n)^{\mathsf{T}} \in \mathbb{C}^n$, and all $\boldsymbol{\nu} = (\nu_1, \nu_2, \ldots, \nu_n)^{\mathsf{T}} \in \mathbb{C}^n$, the conditional probability density function of the channel output $\boldsymbol{Y}$ in (7) is given by

$$f_{\boldsymbol{Y}|\boldsymbol{X}}(\boldsymbol{y}|\boldsymbol{x}) = \prod_{m=1}^{n} \frac{1}{\pi\sigma^2} \exp\left(-\frac{|y_m - \nu_m|^2}{\sigma^2}\right). \tag{8}$$

The EH does not down-convert or filter the received input $Z(t)$ (see [13] and [14]). The RF signal $Z(t)$ in (6b) is used as is for harvesting the energy contained in it.

II. Information and Energy Transmission

Within the framework of Section I-A, two tasks must be accomplished: information transmission and energy transmission.

A. Information Transmission

Let $M \leqslant 2^{n \log L}$ be the number of message indices, with L in (2). To reliably transmit a message index, the transmitter uses an (n, M)-code defined as follows.

Definition 1. *(n, M)-code: An (n, M)-code for the random transformation in* (7) *is a system*

$$\{(\boldsymbol{u}(1), \mathcal{D}_1), (\boldsymbol{u}(2), \mathcal{D}_2), \ldots, (\boldsymbol{u}(M), \mathcal{D}_M)\}, \tag{9}$$

where, for all $(i, j) \in \{1, 2, \ldots, M\}^2, i \neq j$,

$$\boldsymbol{u}(i) = (u_1(i), u_2(i), \ldots, u_n(i)) \in \mathcal{X}^n, \tag{10a}$$
$$\mathcal{D}_i \cap \mathcal{D}_j = \phi, \tag{10b}$$
$$\bigcup_{i=1}^{M} \mathcal{D}_i \subseteq \mathbb{C}^n, \text{ and} \tag{10c}$$
$$|u_m(i)| \leqslant P, \tag{10d}$$

where P is the peak-amplitude constraint and $\mathcal{X}$ is defined in (1)*.*

Assume that the transmitter uses the (n, M)-code

$$\mathscr{C} \triangleq \{(\boldsymbol{u}(1), \mathcal{D}_1), (\boldsymbol{u}(2), \mathcal{D}_2), \ldots, (\boldsymbol{u}(M), \mathcal{D}_M)\} \tag{11}$$

that satisfies (10). The results in this paper are presented in terms of the types induced by the codewords of such a code.

Given an $(n, M, \epsilon, B, \delta)$-code $\mathscr{C}$ in (11), the type induced by the codeword $\boldsymbol{u}(i)$, with $i \in \{1, 2, \ldots, M\}$, is a probability mass function (pmf) whose support is equal to or a subset of $\mathcal{X}$ in (1). This pmf is denoted by $P_{\boldsymbol{u}(i)}$ and for all $x \in \mathcal{X}$,

$$P_{\boldsymbol{u}(i)}(x) \triangleq \frac{1}{n} \sum_{t=1}^{n} \mathbb{1}_{\{u_t(i) = x\}}. \tag{12}$$

The type induced by all the codewords in $\mathscr{C}$ is also a pmf on the set $\mathcal{X}$ in (1). This pmf is denoted by $P_{\mathscr{C}}$ and for all $x \in \mathcal{X}$,

$$P_{\mathscr{C}}(x) \triangleq \frac{1}{M} \sum_{i=1}^{M} P_{\boldsymbol{u}(i)}(x). \tag{13}$$

A class of codes that is of particular interest in this study is that of homogeneous codes, which are defined hereunder.

Definition 2 (Homogeneous Codes)**.** *An $(n, M, \epsilon, B, \delta)$-code $\mathscr{C}$ for the random transformation in* (7) *of the form in* (11) *is said to be homogeneous if for all $x \in \mathcal{X}$, it holds that*

$$P_{\boldsymbol{u}(i)}(x) = P_{\mathscr{C}}(x), \tag{14}$$

where, $P_{\boldsymbol{u}(i)}$ and $P_{\mathscr{C}}$ are the types defined in (12) *and* (13)*, respectively.*

The information rate of any (n, M)-code $\mathscr{C}$ is given by $R(\mathscr{C}) = \frac{\log_2 M}{n}$ bits per channel use. To transmit the message index $i \in \{1, 2, \ldots, M\}$, the transmitter uses the codeword $\boldsymbol{u}(i) = (u_1(i), u_2(i), \ldots, u_n(i))$ in (10a). That is, at channel use m, with $m \in \{1, 2, \ldots, n\}$, the transmitter inputs the RF signal corresponding to symbol $u_m(i)$ into the channel. At the end of n channel uses, the IR observes a realization of the random vector $\boldsymbol{Y}$ in (7) with $\boldsymbol{\nu} = \boldsymbol{u}(i)$. The IR decides that the message index i, with $i \in \{1, 2, \ldots, M\}$, was transmitted if the event $\boldsymbol{Y} \in \mathcal{D}_i$ takes place, with $\mathcal{D}_i$ in (11). That is, the set $\mathcal{D}_i \subseteq \mathbb{C}$ is the region of correct detection for message index i. Therefore, the average DEP associated with code $\mathscr{C}$ is given by

$$\gamma(\mathscr{C}) \triangleq \frac{1}{M} \sum_{i=1}^{M} \left(1 - \int_{\mathcal{D}_i} f_{\boldsymbol{Y}|\boldsymbol{X}}(\boldsymbol{y}|\boldsymbol{u}(i)) \mathrm{d}\boldsymbol{y}\right). \tag{15}$$

This leads to the following refinement of Definition 1.

Definition 3 ((n, M, ϵ)-codes)**.** *An (n, M)-code $\mathscr{C}$ for the random transformation in (7) is said to be an (n, M, ϵ)-code if*

$$\gamma(\mathscr{C}) < \epsilon, \tag{16}$$

with $\gamma(\mathscr{C})$ in (15)*.*

B. Energy Transmission

While transmitting message $i \in \{1, 2, \ldots, M\}$, the channel output observed at the EH is denoted by $Z_i(t)$, with $t \in [0, nT]$. From (5) and (6b), the channel output $Z_i(t)$ is given by

$$Z_i(t) = \Re\Big(\sqrt{2} \sum_{m=1}^{n} u_m(i) \operatorname{sinc}\left(f_w(t - (m-1)T)\right) \exp\left(\mathrm{i}2\pi f_c t\right)\Big) + N_2(t) \tag{17}$$
$$= x_i(t) + N_2(t), \tag{18}$$

where, for all $m \in \{1,2,\ldots,n\}$, the complex $u_m(i)$ is the m^{th} symbol of the codeword $\boldsymbol{u}(i)$ in (10a); for all $t \in [0,nT]$, the signal $x_i(t)$ in (18) is

$$x_i(t)=\Re\Big(\sqrt{2}\sum_{m=1}^{n} u_m(i)\,\mathrm{sinc}\left(f_w(t-(m-1)T)\right) \exp\left(\mathrm{i}2\pi f_c t\right)\Big); \tag{19}$$

and the random variable $N_2(t)$ is a real Gaussian random variable with zero mean and variance σ^2 in (8) and it induces the probability measure P_{N_2} on the measurable space $(\mathbb{R},\mathscr{B}(\mathbb{R}))$. For all $t \in [0,nT]$, the channel output $Z_i(t)$ in (18) is a real Gaussian random variable with mean $x_i(t)$ and variance σ^2.

Due to the presence of non-linear elements such as diodes in the EH circuits, the expected energy harvested from a signal is a function of higher powers of the signal magnitude [14] in addition to the squared magnitude as was conventionally assumed (see [3], [6] and [10]). Recent research on EH non-linearities [13]–[15] has shown that energy models that do not account for these non-linearities result in inaccurate estimates of the harvested energy. In fact, the non-linear energy model in [13], [14] states that the energy harvested from a signal is proportional to the DC component of the second and fourth powers of the signal. Using this model, for all $i \in \{1,2,\ldots,M\}$, the expected energy harvested from the channel output $Z_i(t)$ in (18) during the time $t \in [0,nT]$ is given by the following [14]:

$$e_i = 0.0034\sum_{m=1}^{n}|u_m(i)|^2 + 0.3829\sum_{m=1}^{n}|u_m(i)|^4, \tag{20}$$

where, for all $m \in \{1,2,\ldots,n\}$, the complex $u_m(i)$ is in (10a).

C. Energy Outage Probability

Let W be a random variable that denotes the message index sent during time $t \in [0,nT]$. For all $i \in \{1,2,\ldots,M\}$, the probability of transmitting message index i is $P_W(i) = \frac{1}{M}$. The energy harvested during time $t \in [0,nT]$ is also a random variable E that is equal to e_i in (20) when message $i \in \{1,2,\ldots,M\}$ is transmitted. The conditional probability of harvesting energy e given that message i was transmitted is $P_{E|W}(e|i) = \mathbb{1}_{\{e=e_i\}}$. The probability that energy e is harvested in n channel uses is given by the following:

$$P_E(e) = \sum_{i=1}^{M} P_{E|W}(e|i)\,P_W(i) = \frac{1}{M}\sum_{i=1}^{M}\mathbb{1}_{\{e=e_i\}}. \tag{21}$$

The EOP associated with code $\mathscr{C}$ is defined as follows:

$$\theta(\mathscr{C},B) \triangleq P_E([0,B)) = \sum_{i\in\{j\in\{1,2,\ldots,M\}:e_j<B\}} P_E(e_i) \tag{22}$$

$$= \frac{1}{M}\Big|\{i\in\{1,2,\ldots,M\}: e_i<B\}\Big| = \frac{1}{M}\sum_{i=1}^{M}\mathbb{1}_{\{e_i<B\}}, \tag{23}$$

where, P_E is the probability measure defined in (21) and e_i is defined in (20).

From (23), several interesting insights can be derived about $\theta(\mathscr{C},B)$. The EOP $\theta(\mathscr{C},B)$ can only take discrete values in the set $\{0,\frac{1}{M},\frac{2}{M},\ldots,1\}$. Moreover, for homogeneous codes [11, Definition 4], it holds that $\theta(\mathscr{C},B) \in \{0,1\}$. The following refinement of Definition 3 follows from (22).

Definition 4 ((n,M,ϵ,B,δ)-code)**.** *An (n,M,ϵ)-code $\mathscr{C}$ for the random transformation in* (7) *is said to be an (n,M,ϵ,B,δ)-code if*

$$\theta(\mathscr{C},B) < \delta. \tag{24}$$

III. Code Construction

The process of characterizing an achievable information-energy region for SIET with finite constellations requires the construction of an (n,M)-code $\mathscr{C}$ of the form in (11). The construction of the code begins with the construction of the channel input symbols. Consider a constellation formed by C *layers*, with $C \in \mathbb{N}$. A layer is a subset of symbols in $\mathbb{C}$ that have the same magnitude. For all $c \in \{1,2,\ldots,C\}$, denote by $L_c \in \mathbb{N}$ the number of symbols in the c^{th} layer and let $A_c \in \mathbb{R}^+$ be the amplitude of the symbols in layer c. Denote such a layer by $\mathcal{U}_c(A_c,L_c)$. That is,

$$\mathcal{U}_c(A_c,L_c) \triangleq \{x_c^{(1)},x_c^{(2)},\ldots,x_c^{(L_c)}\}, \tag{25a}$$

where, for all $\ell \in \{0,1,2,\ldots,(L_c-1)\}$,

$$x_c^{(\ell)} = A_c\exp\left(\mathrm{i}\frac{2\pi}{L_c}\ell\right). \tag{25b}$$

Using (25a), the set $\mathcal{X}$ in (1) satisfies

$$\mathcal{X} = \bigcup_{c=1}^{C}\mathcal{U}_c(A_c,L_c). \tag{25c}$$

The vector of the amplitudes in (25c) is denoted by

$$\boldsymbol{A}_c = (A_1,A_2,\ldots,A_C)^{\mathsf{T}}; \tag{25d}$$

and the vector of the number of symbols in each layer in (25c) is denoted by

$$\boldsymbol{L}_c = (L_1,L_2,\ldots,L_C)^{\mathsf{T}}. \tag{25e}$$

The total number of symbols L in (2) for $\mathcal{X}$ in (25c) is $L = \sum_{c=1}^{C}L_c$. Without any loss of generality, assume that $A_1 > A_2 > \ldots > A_C$.

The construction of the (n,M)-code $\mathscr{C}$ is as follows. For all $c \in \{1,2,\ldots,C\}$, let $p_c \in [0,1]$ be the frequency with which symbols of the c^{th} layer appear in the code. The resulting probability vector is denoted by

$$\boldsymbol{p} = (p_1,p_2,\ldots,p_C)^{\mathsf{T}}, \tag{25f}$$

where, for all $c \in \{1,2,\ldots,C\}$,

$$p_c = \frac{1}{Mn}\sum_{i=1}^{M}\sum_{m=1}^{n}\mathbb{1}_{\{u_m(i)\in\mathcal{U}_c\}}, \tag{25g}$$

with $\mathcal{U}_c$ defined in (25a). The symbols within a layer are used with the same frequency in $\mathscr{C}$. Hence, for all $c \in$

$\{1, 2, \ldots, C\}$, the frequency with which the symbol $x \in \mathcal{U}_c(A_c, L_c)$ in (25a) appears in $\mathscr{C}$ is

$$P_{\mathscr{C}}(x) \triangleq \frac{1}{Mn} \sum_{i=1}^{M} \sum_{m=1}^{n} \mathbb{1}_{\{u_m(i)=x\}} = \frac{p_c}{L_c}. \tag{25h}$$

The decoding set $\mathcal{G}_c^{(\ell)} \subseteq \mathbb{C}$ associated with the symbol $x_c^{(\ell)}$ in (25a) is a circle of radius $r_c \in \mathbb{R}^+$ centered at $x_c^{(\ell)}$. That is,

$$\mathcal{G}_c^{(\ell)} = \left\{ y \in \mathbb{C} : \left| y - x_c^{(\ell)} \right|^2 \leq r_c^2 \right\}. \tag{25i}$$

The radii r_1, r_2, ..., r_C are chosen such that the decoding regions are mutually disjoint. To ensure this, for all $c \in \{1, 2, \ldots, C\}$, the amplitudes A_c in (25d) satisfy that

$$A_c - A_{c-1} \geq r_c + r_{c-1}. \tag{25j}$$

The vector of these radii is denoted by

$$\boldsymbol{r} = (r_1, r_2, \ldots, r_C)^{\mathsf{T}}. \tag{25k}$$

The decoding region for the codeword $\boldsymbol{u}(i)$ is

$$\mathcal{D}_i = \mathcal{D}_{i,1} \times \mathcal{D}_{i,2} \times \ldots \times \mathcal{D}_{i,n}, \tag{25l}$$

where, for all $i \in \{1, 2, \ldots, M\}$, $c \in \{1, 2, \ldots, C\}$, $m \in \{1, 2, \ldots, n\}$, and $\ell \in \{1, 2, \ldots, L_c\}$, when $u_m(i) = x_c^{(\ell)}$, then, $\mathcal{D}_{i,m} = \mathcal{G}_c^{(\ell)}$. This defines a family of $(n, M, \epsilon, B, \delta)$-codes denoted by

$$\mathsf{C}\left(C, \boldsymbol{A}_c, \boldsymbol{L}_c, \boldsymbol{p}, \boldsymbol{r}\right), \tag{26}$$

with the number of layers C in (25c), $\boldsymbol{A}_c$ in (25d), $\boldsymbol{L}_c$ in (25e), $\boldsymbol{p}$ in (25f) and $\boldsymbol{r}$ in (25k).

IV. The Information-Energy Region

The information-energy region for finite block-length SIET with finite constellations has been characterized in [11] and [12]. This section summarizes these results and provide improved bounds on the EOP δ that account for the EH non-linearities that are modeled in Section II-B. The following theorem characterizes a converse region for codes in $\mathsf{C}\left(C, \boldsymbol{A}_c, \boldsymbol{L}_c, \boldsymbol{p}, \boldsymbol{r}\right)$ in (26).

Theorem 1. *Consider any homogeneous $(n, M, \epsilon, B, \delta)$-code $\mathscr{C}$ in the family $\mathsf{C}\left(C, \boldsymbol{A}_c, \boldsymbol{L}_c, \boldsymbol{p}, \boldsymbol{r}\right)$ in* (26) *with the constellation $\mathcal{X}$ in* (25c)*. Then, the following hold:*

$$M \leq \frac{n!}{\prod_{c=1}^{C} \left((n\frac{p_c}{L_c})! \right)^{L_c}}; \tag{27a}$$

$$\delta > \frac{1}{M} \sum_{i=1}^{M} \mathbb{1}_{\{e_i < B\}}; \text{ and} \tag{27b}$$

$$\epsilon \geq 1 - \left(1 - \mathrm{Q}\left(\frac{|x^\star - \bar{x}^\star|}{\sqrt{2\sigma^2}} - \frac{\sigma}{\sqrt{2}|x^\star - \bar{x}^\star|} \log\left(\frac{P_{\mathscr{C}}(\bar{x}^\star)}{P_{\mathscr{C}}(x^\star)} \right) \right) \right)^n, \tag{27c}$$

where, the type $P_{\mathscr{C}}$ is defined in (13)*; the real σ^2 is defined in* (8)*; for all $i \in \{1, 2, \ldots, M\}$, the real $e_i \in [0, \infty)$ is in* (20)*; the complex $\bar{x} \in \mathcal{X}$ denotes the nearest neighbor of the symbol $x \in \mathcal{X}$, i.e.,*

$$\bar{x} \in \arg \min_{y \in \mathcal{X} \setminus \{x\}} |x - y|; \tag{28}$$

and $x^\star \in \mathcal{X}$ is such that

$$x^\star \in \arg \max_{x \in \mathcal{X}} \left(1 - \mathrm{Q}\left(\frac{|x - \bar{x}|}{\sqrt{2\sigma^2}} - \frac{\sigma}{\sqrt{2}|x - \bar{x}|} \log\left(\frac{P_{\mathscr{C}}(\bar{x})}{P_{\mathscr{C}}(x)} \right) \right) \right). \tag{29}$$

The function Q *in* (33c) *and* (35) *is the* Q *function defined in [19, Equation* $(2.3 - 10)$*].*

Proof. The proofs of (33a) and (33c) are provided in [20, Section 4] and (33b) follows from (23) and (24). □

The following theorem provides various achievability bounds for codes in the family $\mathsf{C}\left(C, \boldsymbol{A}_c, \boldsymbol{L}_c, \boldsymbol{p}, \boldsymbol{r}\right)$ in (26).

Theorem 2. *A homogeneous (n, M)-code $\mathscr{C}$ in the family $\mathsf{C}\left(C, \boldsymbol{A}_c, \boldsymbol{L}_c, \boldsymbol{p}, \boldsymbol{r}\right)$ in* (26) *is an $(n, M, \epsilon, B, \delta)$-code if the following hold:*

$$L_c \leq \frac{\pi}{2 \arcsin \frac{r_c}{2A_c}}; \tag{30a}$$

$$M \leq \frac{n!}{\prod_{c=1}^{C} \left((n\frac{p_c}{L_c})! \right)^{L_c}}; \tag{30b}$$

$$\delta > \frac{1}{M} \sum_{i=1}^{M} \mathbb{1}_{\{e_i < B\}}; \tag{30c}$$

$$\epsilon \geq 1 - \prod_{c=1}^{C} \left(1 - \exp\left(-\frac{r_c^2}{\sigma^2} \right) \right)^{np_c}, \tag{30d}$$

(30e)

where, for all $i \in \{1, 2, \ldots, M\}$, the real $e_i \in [0, \infty)$ is defined in (20)*.*

Proof. The proofs of (30a), (30b) and (30d) are provided in [20, Section 5.2] and (30c) follows from (23) and (24). □

V. Discussion

Theorems 3 and 2 reveal several interesting insights into the trade-offs between the information transmission rate R, the energy transmission rate B, the DEP ϵ and the EOP δ in SIET. The converse and achievability bounds on R, B, ϵ and δ for a code $\mathscr{C}$ are connected by the type $P_{\mathscr{C}}$ in (13). The lower bound on δ in (33b) and (30c) increases as B increases and vice versa. The consequence of this relationship is that a lower δ can be achieved at the cost of a lower B. Similarly, in order to improve B, a higher value of δ has to be tolerated. The bounds in (33b) and (30c) also reveal that both B and δ can be improved by a code that has higher values of e_i in 20. This is achieved by using the symbols with greater energy more frequently in the code. In fact, for the constructed codes in the family $\mathsf{C}\left(C, \boldsymbol{A}_c, \boldsymbol{L}_c, \boldsymbol{p}, \boldsymbol{r}\right)$ in (26), the largest B and the least δ are achieved by a code with $p_1 = 1$ in (25f).

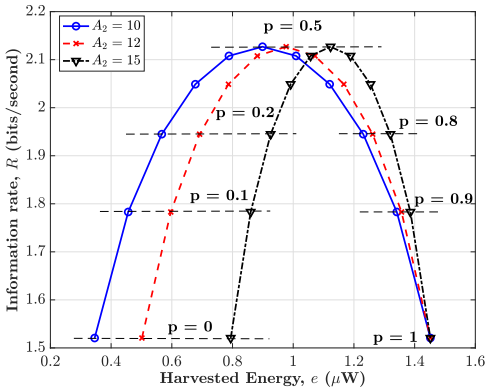

Fig. 1: Converse bounds on the information transmission rate R in (33a) as a function of the harvested energy e in (32).

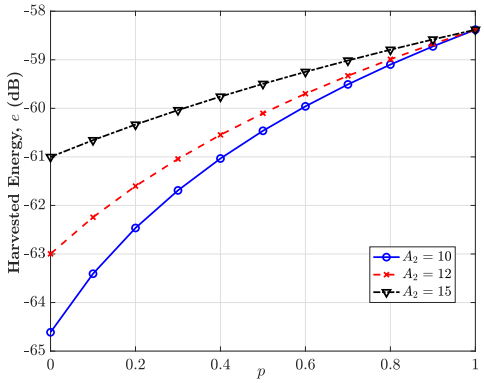

Fig. 2: The bounds on the harvested energy e in (32) as a function of p in (31).

The converse bound on the DEP ϵ in (33c) decreases as a function of the magnitude of the distance between the symbols in the constellation $\mathcal{X}$ in (25c). The achievable bound on ϵ in (30d) decreases as a function of the radii of the decoding regions in (25i). In fact, decreasing the radii of the decoding regions also decreases the distance between the symbols in different layers of $\mathcal{X}$ due to (25j). The number of messages M in (33a) and (30b) and hence the information rate R is maximized by a code with a uniform type $P_{\mathscr{C}}$. More precisely, maximum R is achieved when, for all $c \in \{1, 2, \ldots, C\}$, the type p_c in (25f) is such that $p_c = \frac{L_c}{L}$.

The converse and achievable information-energy rate curves for codes in the family $\mathsf{C}(C, \boldsymbol{A}_c, \boldsymbol{L}_c, \boldsymbol{p}, \boldsymbol{r})$ in (26) are presented in [12, Figure 2]. It is observed that the converse and achievable information-energy rate curves overlap. However, for the same information and energy rate pairs, the DEP for the achievable curves is higher than that for the converse. The sub-optimality in DEP arises due to the sub-optimal choice of circular decoding regions in (25i). The trade-offs between R, B, ϵ, and δ are further illustrated using the following example.

A. Example

Consider a homogeneous $(n, M, \epsilon, B, \delta)$-code $\mathscr{C}$ in the family $\mathsf{C}(C, \boldsymbol{A}_c, \boldsymbol{L}_c, \boldsymbol{p}, \boldsymbol{r})$ in (26) with the peak-amplitude constraint $P = 20$ millivolts in (10d). The constellation $\mathcal{X}$ in (25c) is

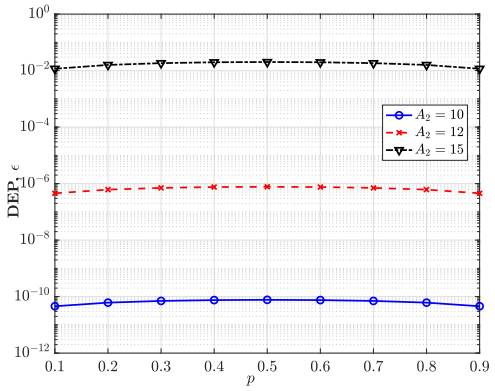

Fig. 3: The bounds on the DEP ϵ in (33c) as a function of p in (31).

composed of two layers with 5 symbols in each layer, *i.e.*, $C = 2$ and $L_1 = L_2 = 5$. The radius of the first layer is $A_1 = P$ and the radius of the second layer A_2 is varied to illustrate the trade-offs between various parameters of $\mathscr{C}$. The frequency with which symbols from the first layer appear in the code is $p_1 = p = 1 - p_2$. That is,

$$\boldsymbol{p} = (p, (1-p))^{\mathsf{T}}. \tag{31}$$

The duration of the transmission in channel uses is $n = 100$. Since $\mathscr{C}$ is a homogeneous code, for all $i \in \{1, 2, \ldots, M\}$, it holds that for some $e \in [0, \infty)$,

$$e_i = e, \tag{32}$$

where e_i is in (20).

Figure 1 shows the trade-offs between the information transmission rate R and the harvested energy e in microwatts (μW) in (32) as a function of p in (31). Each curve in the figure is generated for some value of $A_2 < A_1$ by varying the value of $p \in [0, 1]$. The following trade-offs can be observed from this figure. The harvested energy e increases as p increases. This is because higher p corresponds to the symbols from the first layer $c = 1$ which have higher energy being used more frequently in $\mathscr{C}$. For a fixed value of A_2 in Figure 1, the information rate R first increases and then decreases as a function of e. For each of the curves, the maximum $R = 2.13$ bits/second corresponds to uniform type, *i.e.*, $p = 0.5$. For p lesser or greater than 0.5, the bound on R decreases. Moreover, the values of R achieved are independent of the values of A_1 and A_2. This is due to the fact that the information rate R is only a function of the number of codewords M in (33a).

Figure 2 shows the variation of the harvested energy e in (32) as a function of p in (31). The value of e increases as p increases. This is because increasing p means that the symbols from the layer with greater energy, *i.e.*, $c = 1$ are used more frequently in $\mathscr{C}$ which increases the harvested energy.

Figure 3 shows the variation of the DEP ϵ in (33c) as a function of the probability p in (31). It is observed that, as A_2 increases, the bound on ϵ increases. This is because, increasing A_2 causes the separation between the two layers of $\mathcal{X}$ in (25c) to increase which results in an increase in ϵ according to (33c).

REFERENCES

[1] F. Tariq, M. R. A. Khandaker, K.-K. Wong, M. A. Imran, M. Bennis, and M. Debbah, "A Speculative Study on 6G," *IEEE Wireless Communications*, vol. 27, no. 4, pp. 118 –125, Apr. 2020.

[2] L. R. Varshney, "Transporting Information and Energy Simultaneously," in *Proc. IEEE International Symposium on Information Theory (ISIT)*, Toronto, ON, Canada, Jul. 2008, pp. 1612–1616.

[3] S. B. Amor and S. M. Perlaza, "Fundamental Limits of Simultaneous Energy and Information Transmission," in *Proc. International Conference on Telecommunications (ICT)*, Thessaloniki, Greece, May 2016, pp. 1–5.

[4] N. Khalfet and I. Krikidis, "The Capacity of SWIPT Systems over Rayleigh-Fading Channels with HPA," in *Proc. IEEE Information Theory Workshop (ITW)*, Kanazawa, Japan, 2021, pp. 1–6.

[5] P. Grover and A. Sahai, "Shannon Meets Tesla: Wireless Information and Power Transfer," in *Proc. IEEE International Symposium on Information Theory*, 2010, pp. 2363–2367.

[6] S. B. Amor, S. M. Perlaza, I. Krikidis, and H. V. Poor, "Feedback Enhances Simultaneous Energy and Information Transmission in Multiple Access Channels," in *Proc. IEEE International Symposium on Information Theory (ISIT)*, Barcelona, Spain, Jul. 2016, pp. 1974–1978.

[7] ——, "Feedback Enhances Simultaneous Wireless Information and Energy Transmission in Multiple Access Channels," *IEEE Transactions on Information Theory*, vol. 63, no. 8, pp. 5244–5265, 2017.

[8] N. Khalfet and S. M. Perlaza, "Simultaneous Information and Energy Transmission in the Two-User Gaussian Interference Channel," *IEEE Journal on Selected Areas in Communications*, vol. 37, no. 1, pp. 156 –170, Jan. 2019.

[9] S. M. Perlaza, A. Tajer, and H. V. Poor, "Simultaneous Information and Energy Transmission: A Finite Block-length Analysis," in *Proc. IEEE International Workshop on Signal Processing Advances in Wireless Communications (SPAWC)*, Kalamata, Greece, Jun. 2018, pp. 1–5.

[10] N. Khalfet, S. M. Perlaza, A. Tajer, and H. V. Poor, "On Ultra-reliable and Low Latency Simultaneous Information and Energy Transmission Systems," in *Proc. IEEE International Workshop on Signal Processing Advances in Wireless Communications (SPAWC)*, Cannes, France, Jul. 2019, pp. 1–5.

[11] S. U. Zuhra, S. M. Perlaza, and E. Altman, "Simultaneous Information and Energy Transmission with Finite Constellations," in *Proc. IEEE Information Theory Workshop (ITW)*, Kanazawa, Japan, Oct. 2021, pp. 1–6.

[12] S. U. Zuhra, S. M. Perlaza, H. V. Poor, and E. Altman, "Achievable Information-Energy Region in the Finite Block-Length Regime with Finite Constellations," in *Proc. IEEE International Symposium on Information Theory (ISIT)*, Espoo, Finland, Jul. 2022.

[13] B. Clerckx and E. Bayguzina, "Waveform Design for Wireless Power Transfer," *IEEE Transactions on Signal Processing*, vol. 64, no. 23, pp. 6313–6328, 2016.

[14] B. Clerckx, "Wireless Information and Power Transfer: Nonlinearity, Waveform Design, and Rate-Energy Tradeoff," *IEEE Transactions on Signal Processing*, vol. 66, no. 4, pp. 847–862, 2018.

[15] M. Varasteh, B. Rassouli, and B. Clerckx, "Wireless Information and Power Transfer over an AWGN Channel: Nonlinearity and Asymmetric Gaussian Signaling," in *Proc. IEEE Information Theory Workshop (ITW)*, Kaohsiung, Taiwan, Nov. 2017, pp. 181–185.

[16] B. Clerckx, R. Zhang, R. Schober, D. W. K. Ng, D. I. Kim, and H. V. Poor, "Fundamentals of Wireless Information and Power Transfer: From RF Energy Harvester Models to Signal and System Designs," *IEEE Journal on Selected Areas in Communications*, vol. 37, no. 1, pp. 4–33, 2019.

[17] A. Lapidoth, *A Foundation in Digital Communication*, 2nd ed. Cambridge University Press, 2017.

[18] D. Tse and P. Viswanath, *Fundamentals of Wireless Communication*. Cambridge University Press, 2005.

[19] J. G. Proakis and M. Salehi, *Digital Communications*, 5th ed. McGraw-Hill Higher Education, 2008.

[20] S. u. Zuhra, S. M. Perlaza, H. V. Poor, and E. Altman, "Simultaneous Information and Energy Transmission with Finite Constellations," Inria Sophia Antipolis - Méditerranée, Research Report RR-9409, Jan. 2022. [Online]. Available: https://hal.inria.fr/hal-03230482